

Current efficiency during anodic dissolution of iron to ferrate(vi) in concentrated alkali hydroxide solutions

K. BOUZEK, I. ROUŠAR

Prague Institute of Chemical Technology, Department of Inorganic Technology, 166 28 Prague 6, Czech Republic

Received 18 November 1992; revised 23 April 1993

The dependence of the current efficiency for oxidation of an iron anode to ferrate(vi) ions in 14 M NaOH was measured in the region of free convection. The highest current yield of 40% was obtained at a current density of 2.1 mA cm^{-2} and temperature of 30°C . The iron anode was activated by cathodic prepolarization. The iron concentration in low oxidation states in solution was determined as 0.13 ± 0.1 and $0.29 \pm 0.25 \text{ g Fe dm}^{-3}$ at 20 and 30°C , respectively. The steady state anodic polarization curves of iron in the transpassive potential region are shifted to lower potential values with increasing NaOH concentration from 11 to 17 M. At 40°C all the curves show a limiting current density around 660 mV vs Hg/HgO, namely 9 and 23 mA cm^{-2} at NaOH concentrations of 11 and 17 M, respectively.

1. Introduction

The formation of ferrate(vi) ions by anodic oxidation of iron in concentrated hydroxide solutions was first observed by Poggendorf [1], and later by Haber [2] and Pick [3]. They found that a necessary condition for the formation of ferrate(vi) is that the pH of the solution be at least 14. The results were better in NaOH solutions than in KOH; the current yield generally increased with the concentration and temperature (from 40 to 50% NaOH or KOH and from 30 to 70°C). The current yield also increased with the content of carbon in the iron used (15.4% for raw iron, 27.8% for steel, and 50.4% for cast iron at a current density of 1 mA cm^{-2} and NaOH concentration of 16.5 M). According to the authors [2, 3], cathodic polarization was the best pretreatment of the anode prior to oxidation. The optimum current density and electrolyte temperature were determined later by Toušek as 3.6 mA cm^{-2} and 20 – 25°C , respectively, with decreasing current density the current efficiency decreased rapidly to zero, whereas with increasing current density, above the optimum, there was only a slow decrease. Different results were found by Pick [3] and Beck *et al.* [7], according to whom the current efficiency increased with the temperature from 10 to 70°C ; however these authors did not indicate the dependence on the current density.

Wrońska [5] and Beck *et al.* [7] studied the stability of aqueous ferrate(vi) solutions; the kinetics of decomposition were described by a first order equation with respect to ferrate(vi). The reaction mechanism for the formation of ferrate(vi) has been discussed by several authors [4, 6, 7].

The influence of pretreatment of the iron anode on the yield of ferrate(vi) and the range of optimum current densities could not be found from the literature [1–4, 6, 7]. Data on the presence of iron in lower

oxidation states than +6 besides ferrate(vi) are scarce [7].

The aim of the present work was to measure the yield of ferrate(vi) under various conditions, to study its decomposition kinetics, and to follow the presence of lower valency states of iron besides ferrate(vi).

2. Experimental details

2.1. Chemicals

A solution of 14 M NaOH, at 20°C , was used in all measurements of current yields. Polarization curves were measured in 11, 14, 17 M NaOH. Sodium hydroxide (Spolana Neratovice) contained the following maximum impurities (in wt %): Cl 0.008, Ag 0.002, Fe 0.002, Al 0.002, PO_4^{3-} 0.005, and Ca^{2+} 0.001.

The content of ferrate(vi) was determined by the chromite method, which is suitable for solutions that are not appreciably contaminated by oxidants [8, 9]. The total iron content was determined by the Zimmermann–Reinhardt method. The iron electrodes were in the form of tubes of 0.6 cm outer diameter and 14 cm length, made of soft iron containing (in wt %) 0.08 C, 0.36 Mn.

2.2. Apparatus

The electrolyser is shown schematically in Fig. 1. Two polymethylmetacrylate glass frames formed the anodic and cathodic compartments separated by a PVC diaphragm (D) 4 cm in width and 13 cm in height, of porosity 43.4% and medium pore size $28 \mu\text{m}$ (Eilenburger Chemie–Werk GmbH, Germany). The diaphragm thickness was 1 mm. The gasket was made of nonvulcanized rubber. The influence of polymethylmetacrylate used for frames on the current yields (e.g. the problem of extraction of soluble

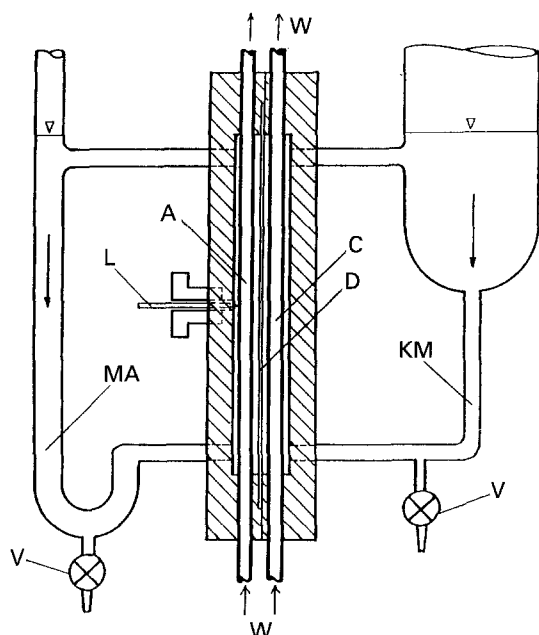


Fig. 1. Scheme of the electrolyser. (A) anode, (C) cathode, (MA) external loop for anolyte, (KM) external loop for catholyte, (D) PVC diaphragm, (V) outlet, (W) in- and outlet of thermostating water, (L) Luggin capillary.

organic compounds into the solution) was negligible. The repeated experiments with new frames and frames after two years of experimental work showed the same current efficiency for the same conditions. There was no visible change in the surface appearance of polymethylmetacrylate parts of the apparatus immersed in the electrolyte after two years of experimental work. Two iron tubes of 0.6 cm outer diameter and 13 cm in length passed through each of the two frames and served as electrodes, which were connected to a water thermostat enabling the temperature to be maintained in the interval 20–70 °C. The Luggin capillary touched the front side of the electrode surface and the ohmic drop between the Luggin capillary and the electrode surface was less than 2 mV for 40 A cm⁻². A HgO/Hg electrode in the same NaOH solution served as a reference. The electrolyte volume was 80 ml in the anode compartment and 140 ml in the cathode compartment (a larger bubble separator).

3. Results and discussion

3.1. Influence of electrode pretreatment on current efficiency

A suitable pretreatment of the anode, especially by cathodic polarization, is known to enhance the current yield [2]. After electrolysis the ferrate(VI) content in the anolyte was determined and the integral current yield was calculated. In all experiments, the electrode was prepolarized cathodically for 30 min at a current density of 20 mA cm⁻². Three runs were carried out, differing by the delay after cathodic activation of the iron anode. In the first run, the delay

was 120 s and the mean current yield was 15% ± 4% at a current density of 10 mA cm⁻² and duration of electrolysis 180 min. In the second run the delay was shortened to or below 10 s, the current yield was 18 ± 3% under the same conditions and, finally, when it was shortened to or below 0.1 s then the current yield was 24% ± 1%. Since this method of activation led to the highest current yield, it was used in all further experiments.

Thus, the positive effect of cathodic prepolarization [2] was substantiated and a favourable influence of shortening the time delay between the end of prepolarization and the start of electrolysis was found.

In accord with the literature [10, 11], it can be assumed that the surface of the iron electrode is freed from an oxide film by the cathodic pretreatment, resulting in a layer of porous active iron that is well ion-permeable. If the cathodic polarization is switched off, the activated iron electrode surface begins to oxidize and gradually passivates.

3.2. Dependence of the current yield on anodic current density

The dependence of the current yield of ferrate(VI) formation on the current density at 20 and 30 °C is shown in Figs 2–4. The decrease of the current yields with increasing current density is at variance with [4], where the current yield passes through a flat maximum in the region of current densities 0.5–5 mA cm⁻², and the optimum is given at $j = 3.6$ mA cm⁻². Below 0.5 mA cm⁻², the data in [4] decrease rapidly. This can be attributed to the fact that the charge passed in 60 min of electrolysis is lower than 1.8 C cm⁻², which is, according to our findings, the lower limit necessary for the formation of ferrate(VI) at 30 °C. Thus, the disagreement between our and Toušek's results [4] can be elucidated.

As can be seen from Figs 2 and 3, the dependence of

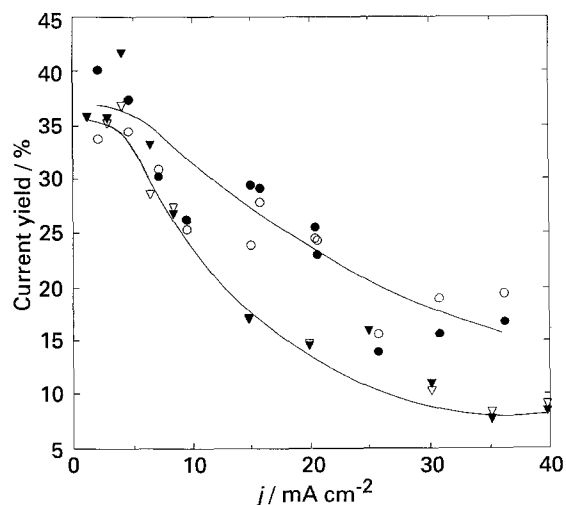


Fig. 2. Current yield with respect to ferrate at various current densities. Concentration of the electrolyte 14 M NaOH, duration of the electrolysis 180 min, (∇) temperature 20 °C, (○) temperature 30 °C. Full symbols (∇, ●) represent repeated experiments.

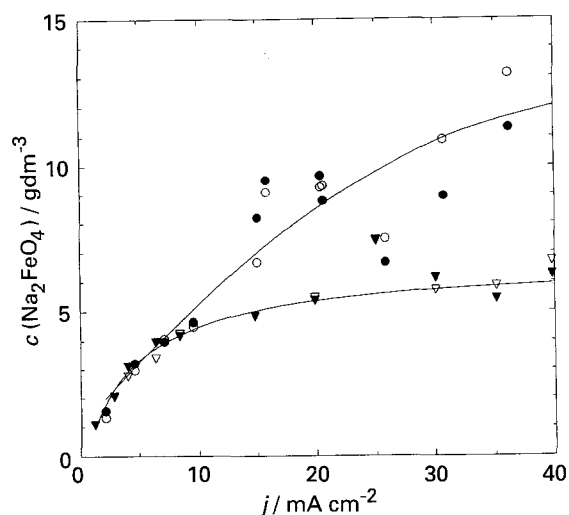


Fig. 3. Concentration of ferrate at various current densities. Concentration of the electrolyte 14 M NaOH, duration of the electrolysis 180 min, (∇) temperature 20°C, (\circ) temperature 30°C. Full symbols (\blacktriangledown , \bullet) represent repeated measurements.

the current yield on temperature becomes pronounced at current densities higher than 8 mA cm^{-2} . Up to this value, the highest increase in current yield is 5% per 10°C . It is probable that the marked dependence on the temperature is due to one or more chemical steps in the reaction mechanism. At low current densities, the concentration of intermediate products in the reaction layer is low. It becomes significant at current densities above 10 mA cm^{-2} and leads to a drop in the current yields at the lower temperature.

The concentration of ferrate(vi) tends to a limiting value (Fig. 3) at various current densities and constant duration of electrolysis, namely about 6 g dm^{-3} at 20°C and 14 g dm^{-3} at 30°C . The difference in current efficiencies is too large to be explained by the increased electrolyte motion due to the increase of the oxygen evolution by natural convection or by an

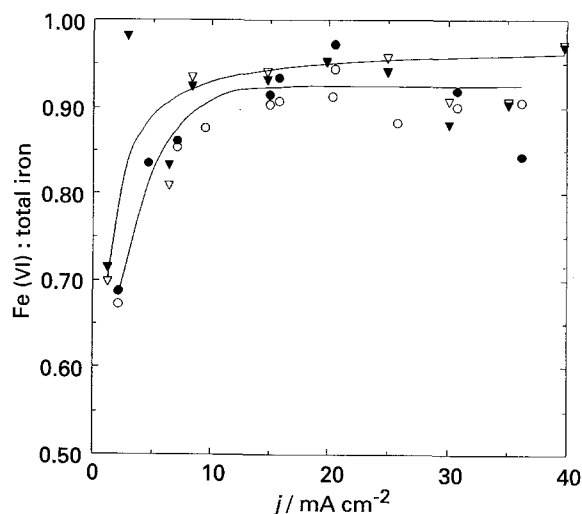


Fig. 4. Ratio of Fe(vi) the total iron content to at various current densities. Concentration of the electrolyte 14 M NaOH, duration of electrolysis 180 min, (∇) temperature 20°C, (\circ) temperature 30°C. Full symbols (\blacktriangledown , \bullet) represent repeated measurements.

increase of the diffusion coefficient with the temperature. Moreover, the agreement of the current yields at low anodic current densities (below 8 mA cm^{-2} at $20\text{--}30^\circ\text{C}$) also suggest the role of a chemical reaction (3) that destroys the passive layer formed during electrolysis on the anode surface [12], enabling further oxidation of iron to proceed. The rate of chemical reaction increased with temperature and OH^- concentration.

It should be noted, however, that it is difficult to predict the behaviour at temperatures beyond the measured interval $20\text{--}30^\circ\text{C}$.

3.3. Dependence of current yield on duration of electrolysis

The dependence of the integral current yield on the duration of electrolysis at a current density of 40 mA cm^{-2} and temperature 20°C is shown in Figs 5 and 6. The number of experimental data is small,

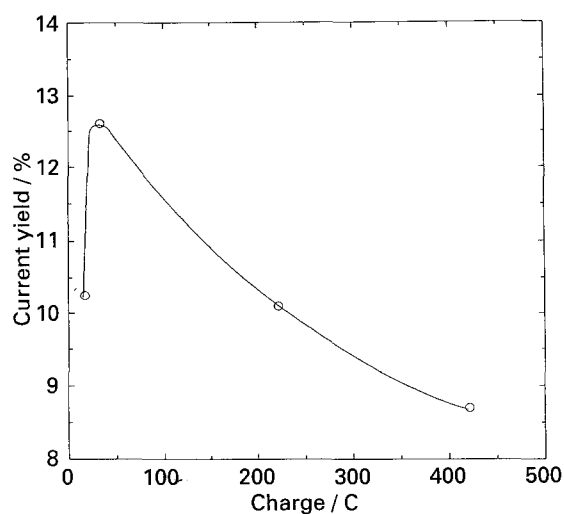


Fig. 5. Current yield with respect to ferrate at various charges. Temperature 20°C , current density 40.0 mA cm^{-2} , concentration of the electrolyte 14 M NaOH.

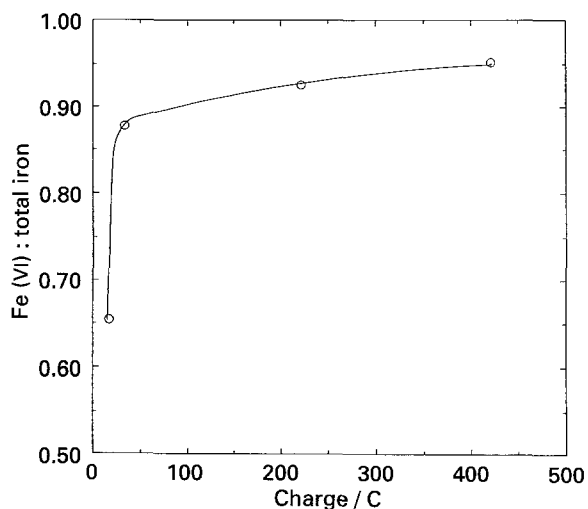


Fig. 6. Ratio of Fe(vi) the total iron content to at various charges. Temperature 20°C , current density 40.0 mA cm^{-2} , electrolyte concentration 14 M NaOH.

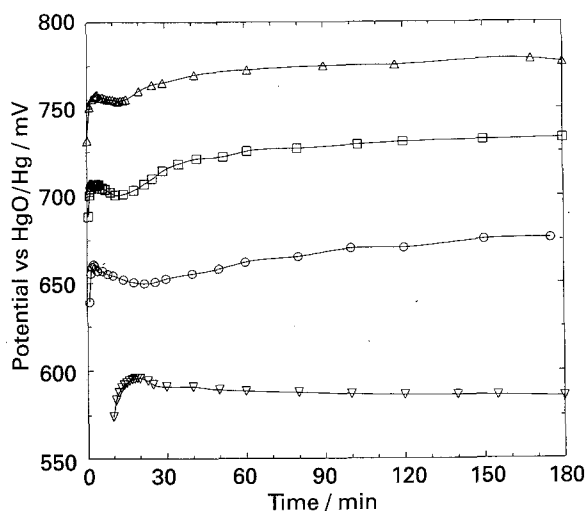


Fig. 7. Anode potential at various times. Current density: (∇) 1.2, (\circ) 8.2, (\square) 20.0 and (Δ) 39.0 mA cm⁻². Temperature 30 °C; electrolyte concentration 14 M NaOH.

but similar results were obtained by Toušek [4] in his Fig. 1.

These results can be explained as follows. During the first several minutes after switching on the current (e.g. 2 min at 8.2 mA cm⁻² or 18 min at 1.2 mA cm⁻²) no formation of ferrate(vi) was visually observed at the anode. The terminal voltage of the electrolyser changed during that time from about 1 to 2.2 V (depending on the current density), when gas evolution commenced and the solution at the anode turned violet due to ferrate(vi) formation. The time after which this voltage was attained is indirectly proportional to the current density and depends on the electrolyte concentration.

The time dependence of the anode potential at various current densities is shown in Fig. 7. The value of the anode potential at which ferrate(vi) formation begins is attained after a certain charge is passed.

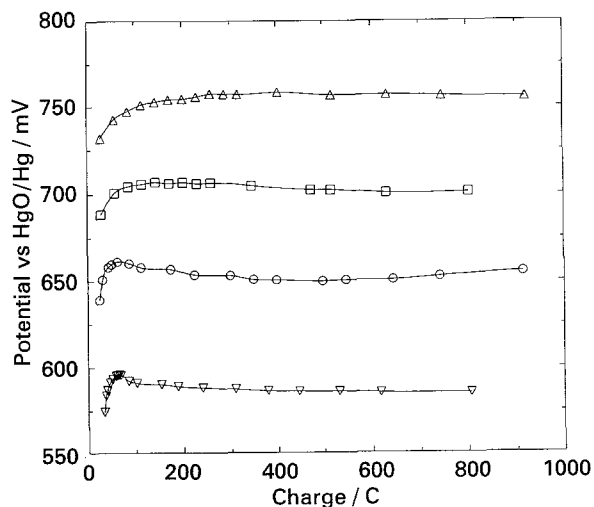
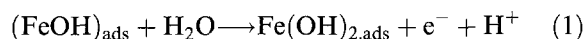


Fig. 8. Anode potential at various charges. Current density: (∇) 1.2, (\circ) 8.2, (\square) 20.0 and (Δ) 39.0 mA cm⁻². Temperature 30 °C, electrolyte concentration 14 M NaOH, the area of anode surface 49 cm², anolyte volume 80 cm³.

This charge was estimated as 1.8 C cm⁻² at 30 °C and 1.3 C cm⁻² at 20 °C, as seen from Fig. 8.

This phenomenon can be explained, e.g. by oxidation of hydrogen adsorbed during the cathodic pre-treatment on the developed electrode surface, or eventually absorbed in the metal. Experimentally it was found that the maximal charge used for the oxidation of adsorbed hydrogen was 0.8 C cm⁻². Alternatively, it may be assumed that intermediate reaction products form, e.g. oxidation of iron to (FeOH)_{ads} [14] and the formation of further oxidation products, e.g. HFeO₂⁻ [15]. These observations led to the proposal of a mechanism of iron dissolution in alkaline solutions (in agreement with [10]), according to which the rate-determining step [7] can be formulated as



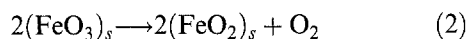
The dependencies shown in Figs 5 and 6 and 1 in [4] suggest that the anodic production of ferrate(vi) can be divided into three steps:

(i) From the start of electrolysis to the start of ferrate(vi) production the intermediate products are formed and also the adsorbed hydrogen is oxidized. In this period the ferrate(vi) current yield is practically zero (a charge of 1.8 C cm⁻² flows across the interface at 30 °C).

(ii) From the start of ferrate(VI) production, simultaneously the development of the passivation of the anode surface and the oxygen evolution started. Considerable surface passivation was reached after passing a charge of approximately 40 C cm⁻² under equal conditions (e.g. constant temperature, current density, electrolyte composition and cathodic pre-treatment), see Fig. 5, corresponding to the current density of 4 mA cm⁻² and duration of electrolysis 180 min. The current yield of ferrate(vi) is about 40%, the integral current yield rises rapidly to a flat maximum (Figs 4, 5, and 1 in [4]).

(iii) The anode surface is subject to increasing passivation, the ferrate(vi) production and the current yield decrease to zero, and the ferrate(vi) concentration remains nearly constant (Figs 2 and 3).

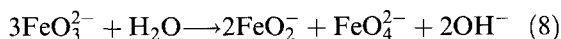
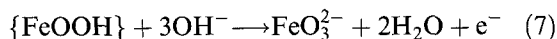
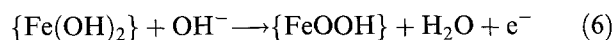
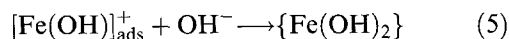
During the second and third steps, as a competing chemical reaction, oxygen evolution is proposed in [2, 3, 6, 7] via ferrate(vi) redox catalysis decomposition according to



The iron concentration in lower oxidation states (ii, iii, iv) remains approximately constant (0.13 ± 0.1 and 0.29 ± 0.25 g Fe dm⁻³ at 20 and 30 °C, respectively). The ratios of these values (0.29/0.13) at 30 and 20 °C is 2.3; the ratio of the limiting ferrate(vi) concentrations attained during measurement of the dependence of current yield on current density is also approximately 2.3.

This supports the assumed mechanism of ferrate(vi) formation, involving HFeO₂⁻ [10], FeO₂⁻ or/and

FeO_4^{4-} as the intermediate products [13]; however, in [7] no intermediate step in the bulk electrolyte is assumed. According to [16] it is possible to assume, that FeO_4^{4-} disproportionates in solution under formation of ferrate(vi) and (III). Following [7, 16, 17] the mechanism of formation of ferrate(vi) can be described by Equations 3–8:



Equations 7 and 8 represent one of the possible reaction schemes of oxidation of ferrate(III) to ferrate(vi).

According to [17–19] the passive layer on the iron surface consists of two sublayers, the inner layer can be identified as Fe_3O_4 and the outer layer consists of oxohydroxides of iron. This outer layer has a lower density than the inner layer and it is not so compact as the inner layer. The brackets in Equations 3 and 4 denote the reaction intermediates whose surface coverage is of the order of a fraction of a monolayer and the braces (Equations 5 and 6) indicate species eventually related to the formation of new phases and which may undergo ageing [17]. The ageing represents a conversion of iron oxohydroxides in the outer layer into Fe_3O_4 . Maintaining constant iron potential in the transpassive region leads gradually to the lowering of the rate of iron dissolution and at the same time to increase in the current density for oxygen evolution; the current yield to ferrate(vi) gradually decreases.

3.4. Polarization curves of iron in NaOH solution

Polarization curves of the iron anode were measured galvanostatically. The anode was prepolarized cathodically at a current density of 20 mA cm^{-2} for 10 min.

The potential corresponding to the current density used was defined as the first maximum on the potential–time curve (Fig. 7), which was most easily reproducible at all current densities. Thus, all potential values corresponded to approximately the same charge passed, namely $1.6\text{--}2.0 \text{ C cm}^{-2}$. After attainment of this point, the formation of ferrate(vi) at the electrode became observable. The electrolyte concentration was 11, 14, and 17 M NaOH and the temperature was 25 and 40 °C. The results are shown in Figs 9 and 10.

A limiting current density was observed at 40 °C in agreement with the literature [3, 7], but not at 25 °C. It was developed in the potential region around 660 mV vs HgO/Hg, and its values were 9, 12, and 23 mA cm^{-2} at concentrations of 11, 14, and 17 M, respectively. Zou and Chin [12] assume that in this region of potentials and concentrations the passive layer at the anode

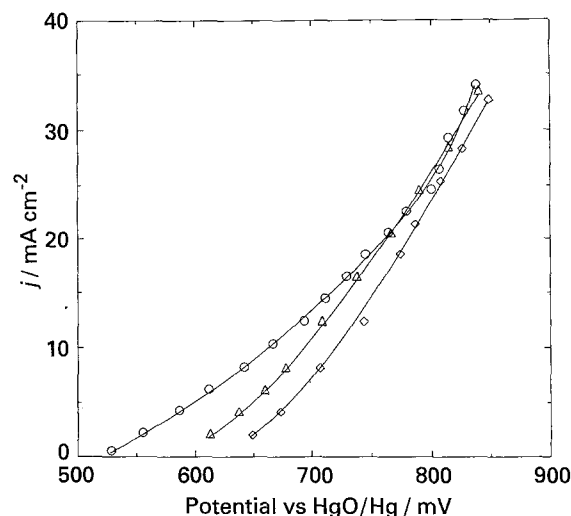


Fig. 9. Steady I - E curves on iron anode. Temperature 25 °C. Electrolyte concentration: (\diamond) 11.0, (Δ) 14.0 and (\circ) 17.0 M NaOH.

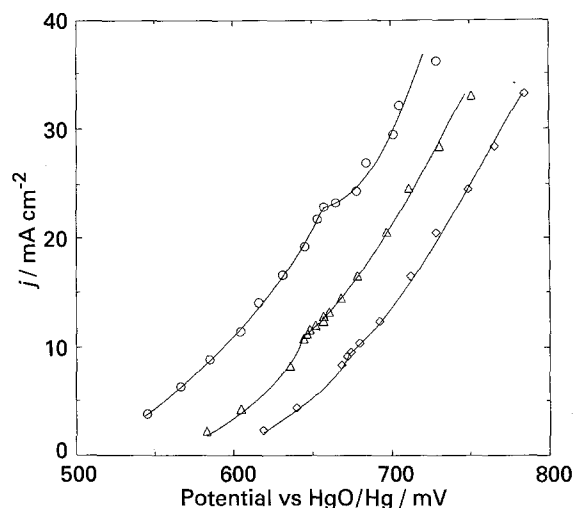


Fig. 10. Steady I - E curves on iron anode. Temperature 40 °C. Electrolyte concentration: (\diamond) 11.0, (Δ) 14.0 and (\circ) 17.0 M NaOH.

surface degrades by the following chemical reaction:

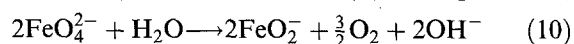


Following Beck [7], it is also possible to assume that in this potential region the oxidation of iron ions from Fe(III) to Fe(IV), Fe(V) and finally Fe(VI) proceeds.

3.5. Decomposition of Na_2FeO_4 in strongly alkaline solution

The obtained solution of ferrate(vi) in 14 M NaOH was stored at 25 °C and samples were taken for analysis at regular intervals. The initial concentration of Na_2FeO_4 was about 5 g dm^{-3} ; the time dependencies are shown in Fig. 11.

The decomposition of the ferrate(vi), see Equation 10,



followed first-order kinetics for a certain time, in

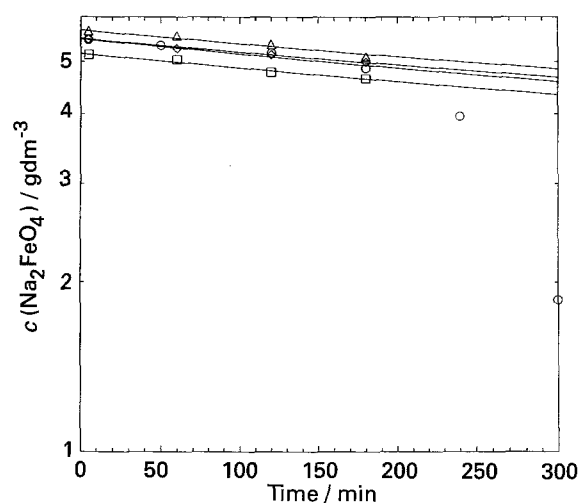


Fig. 11. Time dependence of the ferrate(vi) concentration. Temperature 25 °C, electrolyte concentration 14 M NaOH.

agreement with the theory of Wrońska [5]. Also, in the presence of 0.1 M FeO_2^- , the rate of decomposition followed first-order kinetics, see Fig. 11. In the present case, the decomposition was controlled by a first-order reaction for at least 3 h [5]. The rate constant of this reaction at NaOH concentration of 14 M was $9.7 \times 10^{-6} \text{ s}^{-1}$ at 25 °C. This is in good agreement with [7], where, however, first-order reaction control was found to last for 30–40 h. This difference can be attributed to the fact that the initial ferrate(vi) concentration was only 1×10^{-3} – 2×10^{-3} M in the cited work, whereas in the present case it was about 30×10^{-3} M.

4. Conclusion

The following points can now be made:

(i) The best pretreatment of electrodes for ferrate(vi) production is cathodic polarization at a sufficiently high current density (in the present case 20 mA cm^{-2}) and for a sufficiently long time (30 min). The time

delay between the end of cathodic prepolarization and the start of ferrate(vi) production must be minimal, preferably less than 1 s.

(ii) The current yield of ferrate(vi) decreases with increasing current density from 1.2 to 40 mA cm^{-2} . The ferrate(vi) concentration increases with current density to a limiting value, of 6 or 14 g dm^{-3} at 20 or 30 °C, respectively. This difference vanished at current densities up to 6 mA cm^{-2} (Figs 2 and 3). The results suggest that the rate of ferrate(vi) formation is limited by a chemical step, as assumed by other authors [7, 10].

(iii) The decomposition of ferrate(vi) during the first 3 h after electrolysis appears to be a first-order reaction with a rate constant of $0.97 \times 10^{-5} \text{ s}^{-1}$ at 25 °C at a concentration of NaOH of 14 M in agreement with [5, 7].

References

- [1] J. C. Poggendorf, *Pogg. Ann.* **54** (1841) 161.
- [2] F. Haber, *Z. Elektrochemie* **7** (1900) 215.
- [3] W. Pick, *ibid.* **7** (1901) 713.
- [4] J. Toušek, *Coll. Czech. Chem. Comm.* **27** (1962) 914.
- [5] M. Wrońska, *Bull. Acad. Polon. Sci., ser. Sci. Chim. Geol. et Geographie* **7** (1959) 137.
- [6] G. Grube and H. Gmelin, *Z. Elektrochemie* **26** (1920) 153.
- [7] F. Beck, R. Kaus and M. Oberst, *Electrochim. Acta* **30** (1985) 173.
- [8] Z. Valtr, J. Toušek and A. Toušková, *Chem. zvesti* **11** (1957) 30.
- [9] O. Petira, PhD thesis VŠCHT, Prague (1985).
- [10] D. M. Dražič and Chen Shen Hao, *Electrochim. Acta* **27** (1982) 1409.
- [11] T. Zakroczyński and Z. Sklarska-Smialovska, *J. Electrochem. Soc.* **132** (1985) 248.
- [12] J.-Y. Zou and D.-T. Chin, *Electrochim. Acta* **33** (1988) 477.
- [13] N. S. Kopelev, Yu. D. Perfiliev and Yu. M. Kiselev, *J. Radioanal. Nucl. Chem.* **157** (1992) 401.
- [14] G. T. Burstein and D. H. Davis, *J. Electrochem. Soc.* **128** (1981) 33.
- [15] H. Neugebauer, G. Nauer and N. Brinda-Konopík, *J. Electroanal. Chem.* **122** (1981) 381.
- [16] W. Levason and C. A. McAuliffe, *Coordinat. Chem. Rev.* **12** (1974) 151.
- [17] R. S. Schrebler Guzmán, J. R. Vilche and A. J. Arvia, *Electrochim. Acta* **24** (1979) 395.
- [18] A. Hugot-Le Goff, J. Flis, N. Boucherit, S. Joiret and J. Wilinski, *J. Electrochem. Soc.* **137** (1990) 2684.
- [19] H. Graham Silver and E. Lekas, *ibid.* **117** (1970) 5.